Acta Biomed 2016; Vol. 87, Supplement 3: 20-27 © Mattioli 1885

Review

Use of DWI in identification of small solid pancreatic focalities (≤ 2 cm)

Francesco Negri[1], Nicola Emanuele Bono[1], Sandro Barbalace[1], Vincenzo Trunfio[1], Silvia Lana[1], Chiara Ganazzoli[1], Emanuela Angela Marcantoni[1], Marilina Totaro[2], Manuela Vallara[1], Raffaele Parziale[1], Daniele Borgia[3]

[1] Department of Surgical Sciences, Section of Radiological Sciences, University of Parma, Parma Hospital, Parma, Italy; [2] University of Ferrara - Morphology, Surgery and Experimental Medicine Dept. - Diagnostic Imaging Section, Ferrara, Italy; [3] ASL Lecce, Italy

Summary. Incidental finding of pancreatic focalities has increased thanks to a larger use of radiological examinations (Ultrasound, CT). The differential diagnosis between focal inflammatory and heteroplastic disease is frequently complicated by the wide spectrum of lesions and by the aspecificity of clinical and medical history, as well as of imaging findings. MRI is the second level choice of examination thanks to its higher intrinsic contrast resolution and parametric capability (1); furthermore, the use of Diffusion Weighted Imaging (DWI) sequences provides additional diagnostic informations. (www.actabiomedica.it)

Key words: DWI sequences, pancreatic focalities, early diagnosis

Diffusion Weighted Imaging sequences

DWI is a recent improvement in tissue characterization capacity, which provides functional information based on H_2O molecules movements in intra and extracellular spaces and across cytoplasmic membrane, in order to produce high intrinsic contrast images (3).

These sequences (spin echo T2-weighted modified) are acquired with different degree of dependence to diffusion signal, according to both span and duration of the gradient applications as well as the time interval between them.

These variables are summarized by the numeric value of a quantitative index known as b factor (sec/mm^2); higher values of b factor cause T2 weighting to decrease while diffusion weighting to increase.

In parenchymatous organs (which in physiological conditions present an isotropic pattern of diffusivity) with b values of 500, the contribution of diffusion sequence is moderate and T2 effects prevails; between 500 and 700 the diffusion weighted increases further, while images obtained with b 800-000 are strongly diffusion weighted.

Tissues with free diffusion (low cell densities, cystic lesions, colliquative necrosis, angiomas) show hyperintensity for low to intermediate b values; at the same time, the signal intensity reduces as the b value increases (3-5).

In particular, for images obtained with low and intermediate b values (50-700), the signal depends on both T2 and perfusion effects, the latter reflecting molecular movements within the microcirculation vascular system.

Tissues with restricted diffusion (inflammation, increased cellular density, fibrosis, cytotoxic oedema, abscesses (coagulation necrosis), mucoproteins, cell size changes and altered membrane permeability, show hyperintensity signal for high b values (800-1000) (3-5).

An increase of cellular density is closely related to a reduction of free diffusion of water molecules,

although not all lesions with positive restriction on DWI are malignancies (Fig. 1).

DWI sequences are obtained using low (between 0 and 50 s/mm^2), intermediate (400-600 s/mm^2) and high b values (800-1000 s/mm^2) according to the diagnostic concern and allow both a qualitative (diffusion-weighted images and apparent diffusion coefficient (ADC) map, that represents a parametric figure) and quantitative assessment (map can be evaluated numerically in post processing by calculating apparent diffusion coefficient (ADC) within regions of interest (ROI) for each individual pixel examined (6).

Quantitative analysis is conditioned by the appropriate choice of b values: for example, exclusive use of high b values allows to assess only the contribution made by cellular cramming/fibrosis (restricted diffusion), while free diffusion effects on ADC numeric value are reduced. Furthermore, since different histopathological components (desmoplasia, fibrosis, necrosis, increased cellularity, inflammatory cell infiltration) are present in variable percentages (8-10) within individual examined focality, the quantitative analysis in differential diagnosis between "mass forming focal pancreatitis" (MFFP) and focal pancreatic cancer (PC) is not a reliable parameter (10).

Another aspect to consider is the T2 shine-through: very prolonged T2 relaxation time tissues show hyperintensity signal for higher b values even if diffusion is free (falsely positive restriction).

Thus, valuation of the ADC maps allows to distinguish whether an high signal on diffusion-weighted images is really related to a restricted diffusion or depends on the T2 shine-through effect.

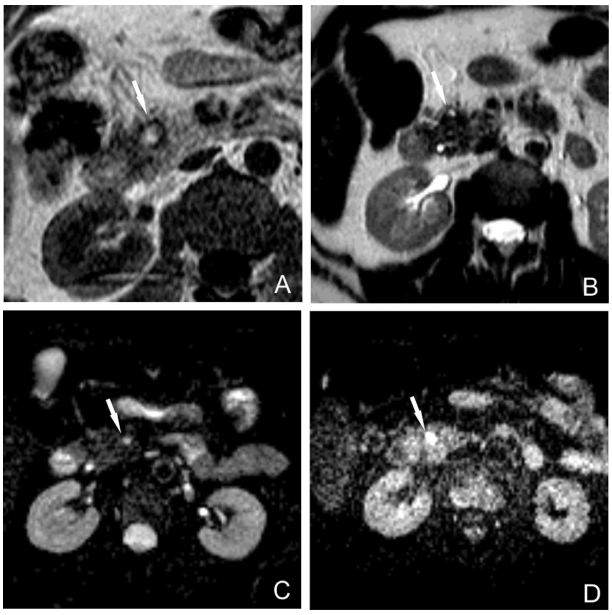

Figure 1. Small cephalopancreatic cyst containing mucoproteins. (A) T1 weighted sequence shows a fluid-fluid level with hyperintensity of declive protein component. (B) Weak hyperintensity of overlying liquid component in T2w sequence. (C-D) DWI sequences with b values 0 and 800 show restricted diffusion due to viscosity contenent (false positive)

For example, in presence of colliquative necrosis, the ADC map allows to identify this artifact by showing a high intensity signal instead of hypointensity, that is indicative of restricted diffusion. The use of DWI sequences in the MRI study protocols still presents a positive cost-benefit ratio because of its low cost and the relative short duration of the acquisition.

Table 1. Pancreatic focal lesions (1, 2, 11)

Non Neoplastic	Neoplastic*
Mass forming focal pancreatitis (MFFP)	Ductal adenocarcinoma
Pseudocyst	NET
Groove pancreatitis	Solid pseudopapillary neoplasm
Pancreatic focal lipomatosis	Pancreatic lymphoma
Intrapancreatic accessory spleen	Pancreatoblastoma
Pancreatic exophytic lobulation	PEComa
Pancreatic sarcoidosis	Serous cystadenoma
	Mucinous cystadenoma
	Intraductal papillary mucinous neoplasm (IPMN)
	Metastasis

Pancreatic focal lesions

Neoplastic lesions of pancreas/periampullary region may arise from the exocrine or endocrine glandular component, the pancreatic ductal epithelium, the bile duct epithelium, the Vater papilla and from the duodenum. Moreover they may be solid (adenocarcinoma, acinar cell carcinoma, NET, pancreatoblastoma) and prone to necrotic-cystic alterations, as well as cystic (serous cystadenoma, mucinous cystadenoma and IPMN) (11).

The biological behavior is variable and an early diagnosis is the only factor able to improve the prognosis in presence of malignant lesions .

Clinical features: frequently absent in presence of accidental injury (for example non secreting NET, focal ADK, accessory intrapancreatic spleen); non specific signs such as vague epigastric tenderness and slight increase of amylase and lipase 8 are sometimes found in presence of focal pancreatitis or pancreatic disagreement secondary to a heteroplastic process.

Focal lesions rarely cause obstructive complications with typical clinical manifestations of chronic pancreatitis, advanced cancer (epigastric pain, jaundice, weight loss) or NET related syndromes (2).

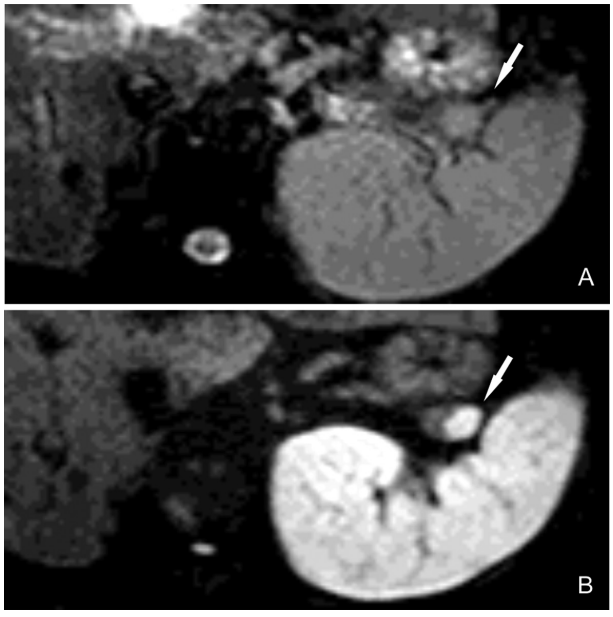

Figure 2. Small accessory spleen of pancreatic tail. (A-B) Diffusion weighted sequences respectively in b0 and b1000 value show gradual increase in signal intensity in parallel to splenic parenchyma

Imaging: MRI aims to characterizing the lesion in order to guide the diagnostic procedure (radiological follow-up vs biopsy); differential diagnosis is complicated because certain lesions are rare and do not show any typical radiological aspect and others (adk, NET) sometimes demonstrate atypical imaging features .

MRI Protocol: envisages axial and coronal Turbo Spin Echo T2 weighted sequences, axial T1 weighted sequences in phase and in opposition phase (T1 dual gradient echo), diffusion-weighted sequences, 2D and 3D cholangiographic sequences (MRCP) to evaluate biliary tree anatomy, T1 weighted sequences (GRE Spoiled 3D) before and after gadolinium intravenous administration (dose of 0.1 mmol/kg, injection rate of 1.5-2 ml/s and injection duration of about 5-8 s) acquired in the arterial, venous and late phase to 20-40 s, 45-65 s, and 3-5 min respectively (16).

ADK: accounts for 85%-95% of malignant pancreatic lesions with prognosis closely related to early diagnosis and generally better before onset of symptoms; the survival rate is approximately <20% at one year and <5% at 5 years).

Pancreatic adenocarcinoma is localized predominantly in head (60-70%), less frequently in body (10-20%) and tail (5-10%), with a males – females ratio of 3:1 and incidence increasing with age (average age at diagnosis of about 71 years).

Risk factors are both hereditary (familiar pancreatic cancer, Peutz-Jeghers, Li-Fraumeni and Linch syndrome, familiar adenomatous polyposis, FAMMM, hereditary pancreatitis and mutations of p16 and BRCA-2), and acquired (old age, cigarette smoking, diabetes mellitus, chronic pancreatitis, alcohol, smoking and obesity).

The most widely used biomarker is CA19.9 with sensitivity of 60-70% and specificity of 70-85% (20). Overall post-operative survival rate at 4 years for patients undergoing resection of small lesions (<2 cm) histologically proven as ductal adenocarcinomas (T1) of pancreas was reported at 78%.

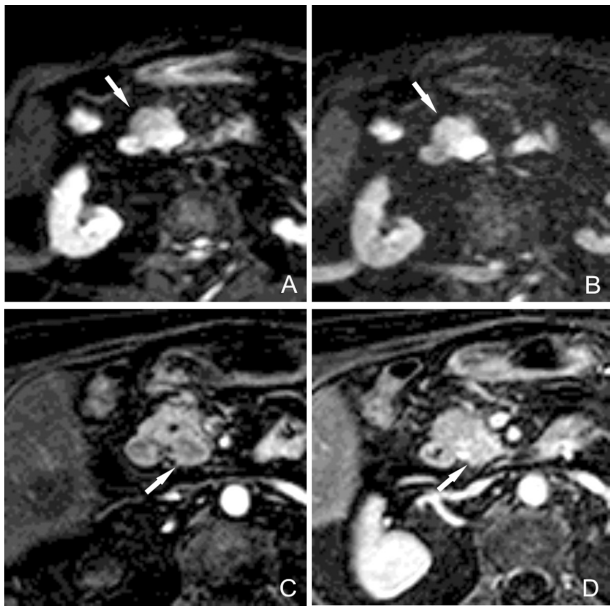

Figure 3. Focal cephalopancreatic ADK. (A) Diffusion-weighted sequence with b200 value shows modest hyperintensity signal riferible to oedematous associated component. (B) Diffusion-weighted sequence with b800 value shows hyperintensity signal indicative of high cellularity/desmoplastic component. (C-D, arterial and late phase respectively) sequences (T1 3D Spoiled GRE) with mdc show progressive enhancement indicative of desmoplastic component

Imaging: adk is usually hypointense both in T1 weighted and T2 weighted sequences, hypovascular in arterial phase with pattern of progressive enhancement in portal and late phase related to its high desmoplastic component (2).

In 10% of cases the contrast enhancement pattern is atypical because it looks isovascular compared to the remaining parenchyma in the portal phase.

In absence of mass effect, alteration of the profile, focal swelling and/or loss of pancreatic lobulation, the indirect signs to be evaluated are: bile ducts and/or Wirsung duct dilatation (double duct sign), atrophy of the parenchyma proximal to the lesion and one or more secondary ducts dilatation. Intralesional cystic-necrotic degeneration is rarely present (8%) (2).

Diffusion-weighted sequences show greater signal intensity for increased b values (800-1000), according to its hypercellularity and desmoplastic stromal component (11).

NET (Neuroendocrine Tumor)

Represent 1-2% of pancreatic neoplasms, more frequently after 50 years old and with slight predominance in males.

There are secreting lesions (causing characteristic syndromes) and non secreting (unrecognized if small); the percentage of malignancy grows with size and is greater in not secreting forms, with malignancy rate between 60% and 92% .

It is possible to find association with MEN 1,Von Hippel-Lindau disease, neurofibromatosis type 1 and tuberous sclerosis.

Table 2. Neuroendocrine Tumors

Tumor	Malignancy	Intrapancreatic location	Signs and Symptoms
Functioning (15-52%)			
Insulinoma	10,00%	90,00%	Hypoglycemia
Gastrinoma	60,00%	25-60%	Zollinger-Ellison syndrome with peptic ulceration and diarrhea
Glucagonoma	70,00%	>90% (prediliction body-tail)	Weight loss, diabetes, diarrhea, migratory erythema
VIPoma	>75%	90% - (prediliction tail)	Werner-Morrison syndrome with diarrhea and ipokaliemia
Somatostatinoma	50,00%	50,00%	Gallstones, weight loss, steatorrhea, diabetes
Non functioning (15-50%)	90,00%	Predidilction for pancreatic head	Abdominal pain and distention, jaundice, weight loss, gastrointestinal bleeding

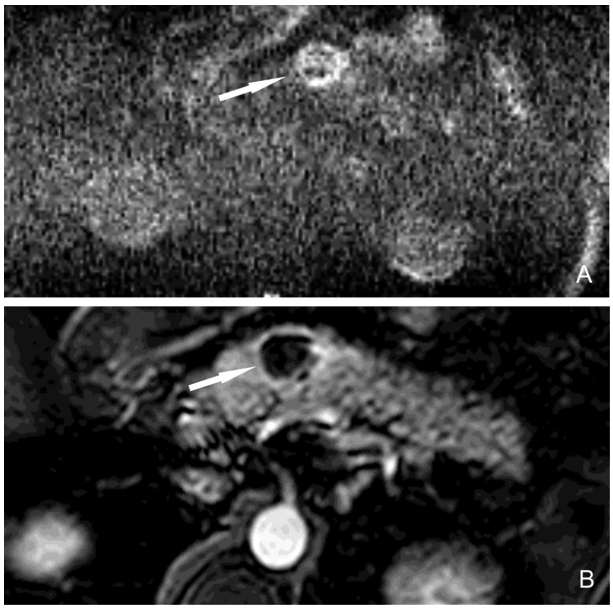

Figure 4. Cystic form of Neuroendocrine tumor (NET). (A) Round cystic lesion of pancreatic isthmus with high signal intensity of wall concentric nodular thickening at 800-b value (reduced signal to noise ratio) as to restricted diffusion. (B) (T1w arterial phase) Intense contrast enhancement of the wall solid component with the central portion of the lesion that shows homogeneous fluid signal

Imaging: typical NETs are hypointense in T1 weighted and hyperintense in T2 weighted images; dynamic sequences show significant arterial wash-in (both secreting and not secreting) with homogeneous enhancement; sometimes show heterogeneous or ring enhancement (necrotico -cystic degeneration is quite frequent). Atypical forms of well differentiated neuroendocrine tumors (benign) have a moderate cellularity and are highlighted for medium-low b values in diffusion-weighted images; in absence of an high vascular component show hypointensity in the arterial phase.

Rarely these tumours in atypical form may contain fibrous intralesional tissue, causing low intensity signal in T2 weighted sequences and lower contrast enhancement in the arterial phase.

Poorly differentiated NET (malignant) are hypercellulated and in diffusion weighted sequences show greater intensity signal for higher b values .

Metastases

Incidence of pancreatic localizations ranges between 3% and 12% in autoptic studies of diffuse metastatic disease. Pancreatic metastases mainly originate from lymphoma, osteosarcoma, melanoma, primitive kidney, lung, gastro-intestinal tract and breast tumours and are almost always associated with disseminated lesions because of their late manifestation (1).

Pancreatic involvement is possible both in cephalopancreatic and body-tail region with solitary (50%-70%), multifocal (5% -10%) or diffuse lesions (15%-44%) (2).

Clinical signs and symptoms are not specific: abdominal pain, weight loss, gastrointestinal bleeding, anemia and diabetic ketoacidosis, while 50%-83% of patients are asymptomatic.

Secondary lesions, arising from renal cell carcinoma (RCC), represent an exception since up to 80% of patients have no metastases in other organs (2).

Imaging: small lesions with well-defined margins usually show hypointensity in T1w and hyperintensity in T2w images; however, signal is variable depending

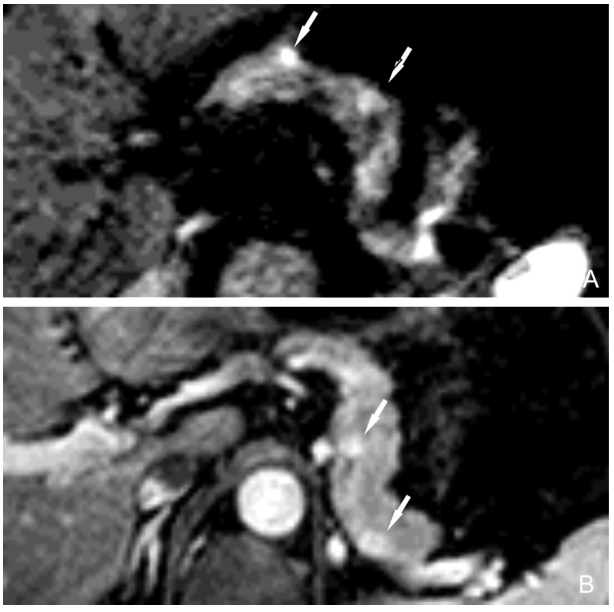

Figure 5. (A) Pancreatic metastases of renal cell carcinoma (RCC) show hyperintensity in diffusion-weighted sequences with b200 value. (B) T1 3D Spoiled GRE with mdc, lesions show high wash-in in arterial phase

on the origin of the tumour and its histological grading. Hypervascular metastases of small dimensions usually have uniform enhancement, while larger lesions may show a ring of peripheral enhancement and central necrotic portion (differential diagnosis with NET necrotic cystic); while hypovascular metastases (lung, breast and colon) present issues of differential diagnosis with adenocarcinoma.

Metastases of renal cell carcinoma (RCC) are typically hypointense in T1w and hyperintense on T2w images with high early wash-in.

Metastases of melanoma differ according to the content of melanin, which has paramagnetic properties, justifying high intensity signal in T1w and isohypointensity in T2w sequences; on the other hand, in presence of amelanotic melanoma, show an iso-hypointensity in T1w sequences.

Focal chronic pancreatitis

It is a focal inflammatory lesion predominantly localized in cephalopancreatic region, which goes into differential diagnosis with adk (it is not uncommon that an inflammatory component is associated to an underlying neoplasm); it is responsible for up to 5% -10% of pancreasectomies for suspect malignancy. Exacerbations lead to a gradual replacement of pancreatic parenchyma with fibrotic tissue and constitute a risk factor for heteroplasia (2% of cases after 10 years and 6% after 20 years). Clinical signs and symptoms such as epigastric pain, obstructive jaundice, weight loss, anemia and modest increase of amylase and lipase are not specific findings.

Imaging: adk and focal pancreatitis have similar signal intensity in T1w and T2 w sequences, in particular, in T1w images there is a focal swelling characterized by hypointensity signal secondary to oedema and fibrosis; in T2 w sequences MFFP shows variable signal intensity: hyperintensity during acute phase caused by lesional edema and adjacent adipose tissue stranding while in chronic phase is predominantly characterized by hypontensity due to fibrosis. In dynamic sequences it is possible to identify a focal hypontensity in arterial phase with progressive wash in during the venous-late phase due to fibrous tissue (22); this behavior is similar to adenocarcinoma because of its desmoplastic component, that usually presents a later peak of enhancement. In lesions with low/absent fibrotic intralesional component, MFFP can show heterogeneous enhancement in arterial phase (9). Indirect signs, although poorly specific, may be useful in differential diagnosis with adenocarcinoma: biliary-pancreatic ducts not dilated crossing the lesion with gradual reduction of caliber ("sign of penetrating duct"), irregularities ("crown of rosary") of main pancreatic duct, calcification and/or moderate parenchymal atrophy suggest a diagnosis of focal pancreatitis (2); on the other hand, abrupt cessation of main pancreatic duct with marked upstream dilatation and atrophy of the parenchyma are more frequent in adenocarcinoma. In addition, a high ratio between Wirsung caliber duct and pancreas width is also highly associated to adenocarcinoma. Obviously, double duct sign, infiltration of peripancreatic adipose tissue, arterial encasement and locoregional venous vessels thrombosis are strongly related with advanced stage of ADK (22).

Focal chronic pancreatitis exacerbation can show restricted diffusion related to high inflammatory in-

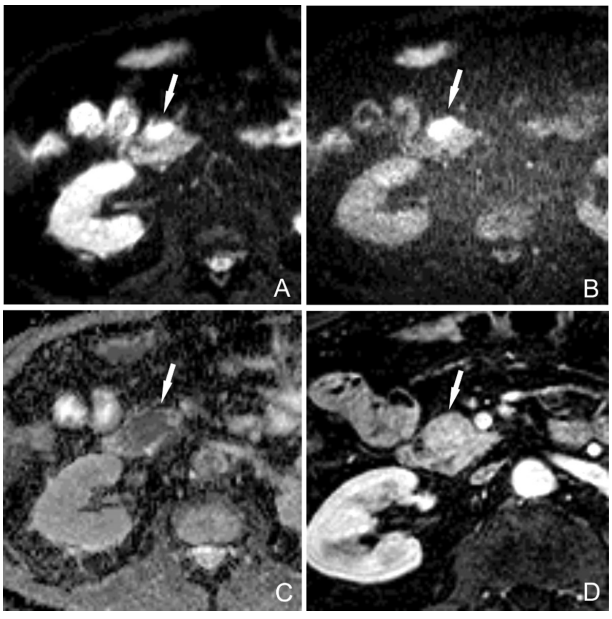

Figure 6. MFFP exacerbation. Diffusion weighted sequences with b100 (A) and b800 (B) respectively show focal hyperintensity of pancreatic head. (C) ADC map confirms restricted diffusion. (D) T1 3D Spoiled GRE with mdc shows progressive enhancement related to presence of a fibrous component of MFFP in venous phase.

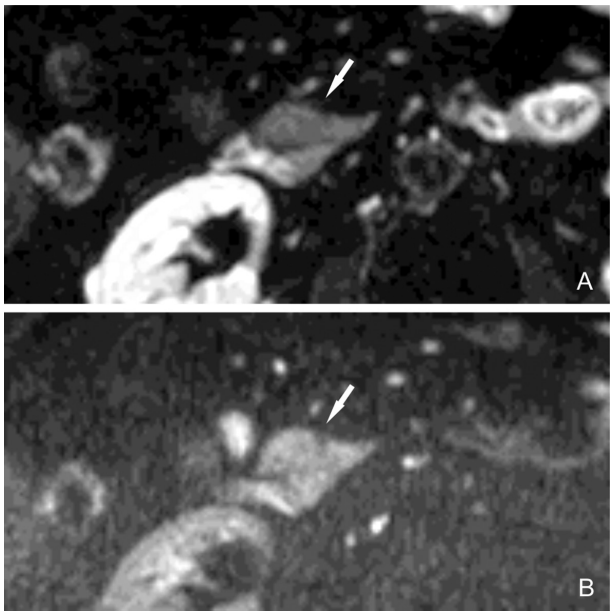

Figure 7. MRI follow-up one month later shows negative findings in diffusion weighted sequences with b100 (A) and b800 value (B), indicating acute phase resolution

filtration and granulation tissue in addition to the fibrotic component (23).

Autoimmune pancreatitis (AIP): represents 25% of focal pancreatitis whose common features are linfoplasmocitary infiltration (as a result of histological exam) and a high level of G4 immunoglobulin in serum. Association with other autoimmune diseases is possible, such as inflammatory bowel disease, primary sclerosing cholangitis and Sjogren's syndrome; clinical and laboratory findings improve after corticosteroids treatment (22).

Imaging: the diffused form shows a generalized glandular enlargement ("sausage shape") and failure of Wirsung duct visualization, while focal variants go into differential diagnosis with adenocarcinoma (2).

Groove pancreatitis: rare form of pancreatitis with unknown pathogenesis located in the pancreatic-duodenal groove, that is a space localized between cephalopancreatic region, duodenal C and main biliar duct. There are two known forms of groove pancreatitis: a segmental form involving pancreatic head and the groove space and a pure form that involves only groove space. Clinically is characterized by the presence of recurrent vomiting caused by duodenal obstruction .

Imaging: groove fibrotic tissue is hypointense in T1w and iso-hypointense in T2w sequence; it shows typical enhancement with progressive wash-in during the dynamic phase, while the segmental form goes into differential diagnosis with adenocarcinoma (7). The smooth stenosis of the intrapancreatic portion of the common bile duct and the thickening with cystic dysplasia of the duodenal wall is considered extrapancreatic signs.

Conclusions

Patients presenting both aspecific clinical information and atypical enhancement pattern may benefit from diffusion weighted sequences which show high sensitivity to small lesions (0.5-1 cm) (25-34) although not always useful in differential diagnosis between heteroplastic lesion and MFFP. In such cases, after therapy, MRI should be performed during follow-up to detect any changes in imaging findings; whenever clinical and radiological findings remain unchanged, bioptic evaluation is required.

References

1. Franz D, Esposito I, Kapp AC, Gaa J, Rummeny EJ. Magnetic resonance imaging of less common pancreatic malignancies and pancreatic tumors with malignant potential. European journal of radiology open 2014; 1: 49-59.
2. Low G, Panu A, Millo N, Leen E. Multimodality imaging of neoplastic and nonneoplastic solid lesions of the pancreas. Radiographics: a review publication of the Radiological Society of North America, Inc. 2011; 31: 993-1015.
3. De Robertis R, Tinazzi Martini P, Demozzi E, et al. Diffusion-weighted imaging of pancreatic cancer. World journal of radiology 2015; 7: 319-28.
4. Malayeri AA, El Khouli RH, Zaheer A, et al. Principles and applications of diffusion-weighted imaging in cancer detection, staging, and treatment follow-up. Radiographics: a review publication of the Radiological Society of North America, Inc. 2011; 31: 1773-91.
5. Morani AC, Elsayes KM, Liu PS, et al. Abdominal applications of diffusion-weighted magnetic resonance imaging: Where do we stand. World journal of radiology. 2013; 5: 68-80.
6. Bozgeyik Z, Onur MR, Poyraz AK. The role of diffusion weighted magnetic resonance imaging in oncologic settings. Quantitative imaging in medicine and surgery 2013; 3: 269-78.

7. Wu LM, Xu JR, Hua J, et al. Value of diffusion-weighted imaging for the discrimination of pancreatic lesions: a meta-analysis. European journal of gastroenterology & hepatology 2012; 24: 134-42.
8. Attariwala R, Picker W. Whole body MRI: improved lesion detection and characterization with diffusion weighted techniques. Journal of magnetic resonance imaging: JMRI 2013; 38: 253-68.
9. Fattahi R, Balci NC, Perman WH, et al. Pancreatic diffusion-weighted imaging (DWI): comparison between mass-forming focal pancreatitis (FP), pancreatic cancer (PC), and normal pancreas. Journal of magnetic resonance imaging: JMRI. 2009; 29: 350-6.
10. Barral M, Sebbag-Sfez D, Hoeffel C, et al. Characterization of focal pancreatic lesions using normalized apparent diffusion coefficient at 1.5-Tesla: preliminary experience. Diagnostic and interventional imaging 2013; 94: 619-27.
11. Wang Y, Miller FH, Chen ZE, et al. Diffusion-weighted MR imaging of solid and cystic lesions of the pancreas. Radiographics : a review publication of the Radiological Society of North America, Inc. 2011; 31: E47-64.
12. Tartaglione T, Visconti E, Botto A, Di Lella GM. Tecniche e metodiche in neuroradiologia, 2014.
13. Yasui O, Sato M. Combined imaging with multi-detector row computed tomography and diffusion-weighted imaging in the detection of pancreatic cancer. The Tohoku journal of experimental medicine 2011; 224: 195-9.
14. Klapman J, Malafa MP. Early detection of pancreatic cancer: why, who, and how to screen. Cancer control: journal of the Moffitt Cancer Center 2008; 15: 280-7.
15. Brenner R, Metens T, Bali M, Demetter P, Matos C. Pancreatic neuroendocrine tumor: added value of fusion of T2-weighted imaging and high b-value diffusion-weighted imaging for tumor detection. European journal of radiology 2012; 81: e746-749.
16. Lee ES, Lee JM. Imaging diagnosis of pancreatic cancer: a state-of-the-art review. World journal of gastroenterology 2014; 20: 7864-77.
17. Laeseke PF, Chen R, Jeffrey RB, Brentnall TA, Willmann JK. Combining in Vitro Diagnostics with in Vivo Imaging for Earlier Detection of Pancreatic Ductal Adenocarcinoma: Challenges and Solutions. Radiology 2015; 277: 644-61.
18. Suzuki R, Ohira H, Irisawa A, Bhutani MS. Pancreatic cancer: early detection, diagnosis, and screening. Clinical journal of gastroenterology 2012; 5: 322-6.
19. Helmstaedter L, Riemann JF. Pancreatic cancer--EUS and early diagnosis. Langenbeck's archives of surgery/Deutsche Gesellschaft fur Chirurgie 2008; 393: 923-7.
20. Wang YX, Gong JS, Loffroy R. On pancreatic cancer screening by magnetic resonance imaging with the recent evidence by Del Chiaro and colleagues. Chinese journal of cancer research = Chung-kuo yen cheng yen chiu 2015; 27: 417-22.
21. Bakir B, Salmaslioglu A, Poyanli A, Rozanes I, Acunas B. Diffusion weighted MR imaging of pancreatic islet cell tumors. European journal of radiology 2010; 74: 214-20.
22. O'Neill E, Hammond N, Miller FH. MR imaging of the pancreas. Radiologic clinics of North America. 2014; 52: 757-77.
23. Takeuchi M, Matsuzaki K, Kubo H, Nishitani H. High-b-value diffusion-weighted magnetic resonance imaging of pancreatic cancer and mass-forming chronic pancreatitis: preliminary results. Acta radiologica 2008; 49: 383-6.
24. Wakabayashi T, Kawaura Y, Satomura Y, et al. Clinical and imaging features of autoimmune pancreatitis with focal pancreatic swelling or mass formation: comparison with so-called tumor-forming pancreatitis and pancreatic carcinoma. The American journal of gastroenterology 2003; 98: 2679-87.
25. Kim H, Lee JM, Yoon JH, et al. Reduced Field-of-View Diffusion-Weighted Magnetic Resonance Imaging of the Pancreas: Comparison with Conventional Single-Shot Echo-Planar Imaging. Korean journal of radiology 2015; 16: 1216-25.
26. De Filippo M, Gira F, Corradi D, et al. Benefits of 3D technique in guiding percutaneous retroperitoneal biopsies. Radiol Med 2011 Apr; 116(3): 407-16. doi: 10.1007/s11547-010-0604-2. Epub 2011 Feb 10.
30. Pescarolo M, Sverzellati N, Verduri A, et al. How much do GOLD stages reflect CT abnormalities in COPD patients? Radiol Med 2008 Sep; 113(6): 817-29. doi: 10.1007/s11547-008-0284-3. Epub 2008 Jul 10.
31. Gafà G, Sverzellati N, Bonati E, et al. Follow-up in pulmonary sarcoidosis: comparison between HRCT and pulmonary function tests. Radiol Med 2012 Sep; 117(6): 968-78. Epub 2012 May 14.
32. Bertolini L, Vaglio A, Bignardi L, et al. Subclinical interstitial lung abnormalities in stable renal allograft recipients in the era of modern immunosuppression. Transplant Proc 2011 Sep; 43(7): 2617-23. doi:10.1016/j.transproceed.2011.06.033.
33. De Filippo M, Onniboni M, Rusca M, et al. Advantages of multidetector-row CT with multiplanar reformation in guiding percutaneous lung biopsies. Radiol Med. 2008 Oct; 113(7): 945-53. doi: 10.1007/s11547-008-0325-y. Epub 2008 Sep 25.
34. De Filippo M, Saba L, Concari G, et al. Predictive factors of diagnostic accuracy of CT-guided transthoracic fine-needle aspiration for solid noncalcified, subsolid and mixed pulmonary nodules. Radiol Med 2013 Oct; 118(7): 1071-81. doi: 10.1007/s11547-013-0965-4. Epub 2013 Jul 25.

Correspondence:
Negri Francesco
Department of Surgical Sciences, Section of Radiological Sciences, University of Parma, Parma Hospital
Via Gramsci, 14 - 43126 Parma (Italy)
E-mail: francesco.negri79@gmail.com